Definition of a Model Fat for Crystallization-in-Emulsion Studies

C. Lopez[a,b], A. Riaublanc[c], P. Lesieur[d], C. Bourgaux[d], G. Keller[a], and M. Ollivon[a,*]

[a]Equipe Physico-Chimie des Systèmes Polyphasés, UMR 8612 du CNRS, 92296 Châtenay-Malabry, France, [b]ARILAIT Recherches, 75314 Paris cedex 09, France, [c]Laboratoire d'Etude des Interactions des Molécules Alimentaires, INRA, 44315 Nantes, France, and [d]Laboratoire pour l'Utilisation du Rayonnement Electromagnétique, Université Paris-sud, 91898 Orsay, France

ABSTRACT: Numerous food products are dispersed in droplet emulsions in which fat is partially crystallized. A model fat allowing the study of crystallization in emulsion, obtained by the mixing of two fats (one solid and one liquid at room temperature) with simple triacylglycerol (TG) composition, is defined and characterized. Cocoa butter (CB), a vegetable fat mainly composed of monounsaturated long-chain fatty acids (POP, POSt, StOSt, where P = palmitic, O = oleic, St = stearic), and miglyol, a synthetic oil made from capric and caprylic fatty acids, were chosen, respectively. The thermal behaviors of CB, miglyol, and their mixtures are studied using high-sensitivity differential scanning calorimetry (DSC). The CB/miglyol ratio was optimized (i) in order to make stable emulsions as a function of time, (ii) so that the mixture displays several solid phases on cooling that result from CB polymorphism, and (iii) in order to keep, even at low temperature, a liquid moiety facilitating the phase transitions. The CB 75%/miglyol 25% composition is defined as the model mixture. This mixture is characterized on cooling at 0.5°C/min by coupled X-ray diffraction as a function of temperature and DSC experiments. First an α 2L (49.3 Å) variety is formed. Then, co-crystallization of both CB and miglyol TG shows the simultaneous formation of longitudinal stackings of 44.5 and 34.5 Å with a lateral organization of β′ form. An unusual TG packing corresponding to compound formation is proposed to explain the observation of a 34.5 Å long-spacing. The crystallization behavior of the model fat mixture dispersed in emulsion droplets is also monitored in order to validate its use.

Paper no. J9926 in *JAOCS 78*, 1233–1244 (December 2001).

KEY WORDS: Cocoa butter, crystallization, DSC, emulsion, triacylglycerols, X-ray diffraction.

In many foods, the fat is dispersed in the form of emulsion, e.g., milk, cream, mayonnaise, butter, and margarine. In most of these emulsions, the fat is partially crystallized. Although this is more sensitive in systems for which fat is the continuous phase (water-in-oil emulsions, like butter and margarine), crystallization inside the droplets of the oil-in-water emulsions influences their organoleptic properties and many of their physical properties, e.g., rheology, stability against aggregation, creaming, and coalescence. Such crystallization plays an important role in the manufacture, storage, transport, and consumption of emulsified food products. Thus, it is of great interest to understand the factors that influence their crystallization behavior.

Whatever their state of dispersion, natural fats are mainly composed of complex mixtures of numerous triacylglycerols (TG) that determine their physical properties, such as texture and plasticity. Milk fat is undoubtedly one of the most complex fats found in nature. TG comprise, by far, the greatest proportion of lipids, making up 97–98% of the total lipid. The other components are diacylglycerols, monoacylglycerols, free fatty acids, sterols, and phospholipids. Over 400 different fatty acids have been identified in milk fat; however only 12 individual fatty acids account for more than 1% (1). Based on all the fatty acids identified, saturated fatty acids account for about 66% (C4:0–C10:0 = 11.2%; C14:0 = 10.8%; C16:0 = 26.1%; C18:0 = 10.8%) of the total, monoenoic acids are 27.4% (C18:1 = 24.1%), dienoic acids are 2.5% (C18:2 = 2.4%), trienoic acids are 1.3% (C18:3 = 1.1%), polyenoic acids are less than 1%, branched acids are less than 2.6%, and miscellaneous acids are less than 1% (1,2). Furthermore, the composition changes with season, region, and cow feeding. Milk fat contains several hundred different TG, among which only 43 TG are present in quantities greater than 0.5% (mol/mol), indicating that the majority of TG are present only in trace amounts (1).

Due to its composition, the melting range of milk fat is broad, spanning from about –40 to 40°C. In this temperature range, a mixture of solid and liquid phases coexists. Previous works (3–11) reported that milk fat consists of several solid phases made from the major groups of glycerides that melt and crystallize separately and that generally behave as independent solid solutions. A typical melting curve of untempered native milk fat determined by differential scanning calorimetry (DSC) shows three endothermic peaks, corresponding to high-, medium-, and low-melting fractions that are chemically distinct (4). The existence of a polymorphism further increases the complexity of milk fat studies. This, added to the existence of a complex membrane (12) in milk, likely results in that only few studies exist on crystallization of milk fat dispersed in emulsion (13–17).

To study crystallization in emulsion droplets, authors use hydrocarbons, such as *n*-hexadecane (18,19), pure TG, or

*To whom correspondence should be addressed at Equipe Physico-Chimie des Systèmes Polyphasés, UMR 8612 du CNRS, 5 rue J.B. Clément, 92296 Châtenay-Malabry, France. E-mail: michel.ollivon@cep.u-psud.fr

simple mixtures of synthetic TG (20) rather than natural fats because they can be obtained with higher purity and display sharp melting and crystallization temperatures. The drawback of the studies made from these simplified models is that they are far from food fat compositions and direct applications. For instance, the coexistence of both solid and liquid phases is a prerequisite for the definition of a milk fat model. According to our requirements, a model for crystallization in emulsion studies should (i) have a limited number of TG in order to facilitate data interpretation, (ii) be available in large quantity for a reasonable price, and (iii) display a weak intersolubility of the two fats, to increase the domain of coexistence of the two phases. A mixture of cocoa butter (CB) and miglyol, a medium-chain length synthetic fat, fulfils these requirements.

CB is a natural fat that has a quite simple composition, even compared to that of other vegetable fats. CB is mainly composed of TG (97%), other components being diacylglycerols (~1.3%), free fatty acids (~1.2%), and complex lipids such as glycolipids (~0.5%) and phospholipids (~0.1%) (21). CB is composed of a mixture of saturated, monounsaturated, and polyunsaturated TG. The monounsaturated TG are by far the major component since they represent about 80% of the total. Moreover, only three TG account for more than 95% of this fraction: 1,3-palmitoyl-2-oleoylglycerol (POP), 1-palmitoyl-2-oleoyl-3-stearoylglycerol (POSt), and 1,3-stearoyl-2-oleoylglycerol (StOSt). Polyunsaturated and trisaturated TG correspond to about 13 and 3%, respectively, of the TG content. This TG composition of CB leads to thermal transitions over a narrower temperature range than that of milk fat. CB forms a hard solid at room temperature and exhibits sharp melting just below body temperature. This TG composition gives CB a thermal and structural behavior comparable to that of a pure compound. This specificity of CB could be used through the identification of crystalline species formed in emulsion, to study the mechanisms of fat crystallization in dispersed systems.

Many authors studied crystallization and polymorphism of CB (22–24) and of its main monounsaturated TG: POP, POSt, and StOSt (25,26). CB polymorphism is commonly described in the literature in terms of six different polymorphic forms, noted from I to VI in increasing order of melting points, according to the nomenclature of Wille and Lutton (22). The solid phases of CB are identified by means of characteristic X-ray diffraction (XRD) peaks. The longitudinal stackings of molecules in lamellae, identified from the long-spacings observed by XRD at small angles, are commonly double or triple chain length (2L or 3L). The specific lateral packing of the fatty acid hydrocarbon chains recorded by XRD at wide angles leads to strong and characteristic short-spacings resulting from the combination of the lateral organization in the different moieties of the monounsaturated molecules. Polymorphs are usually divided into three groups: α (hexagonal subcell), β′ (orthorhombic subcell), and β (triclinic subcell), in their order of subcell compactness. In fact, CB polymorphism is more complex than originally described. At room temperature, three phases coexist. The main one, composed mainly of monounsaturated TG, is solid, and a minor one corresponding mainly to saturated TG coexists with a liquid phase representing 25% at 22°C and 33% at 27–28°C that is mainly composed of polyunsaturated TG (in which a small quantity of the other TG, varying with temperature, is solubilized). A liquid crystalline phase has also been identified upon quenching of CB to low temperature (24).

The aim of this paper is to define and characterize, by high-sensitivity DSC and X-ray diffraction as a function of temperature (XRDT) experiments, a model fat allowing the study of crystallization in emulsion. In order to obtain a mixture of liquid and solid TG, as can be found in naturally occurring products such as milk and cream, the long-chain TG of CB were blended with various proportions of miglyol, which is a synthetic mixture of medium-chain TG made from caprylic and capric acids. The study by the above techniques of a selected mixture of these two fats in emulsion validates the model used.

MATERIALS AND METHODS

Samples. The CB used was a standard factory product originating from Ivory Coast (Barry Callebaut, Meulan, France). Miglyol was purchased from Stearinerie Dubois fils (Ciron, France).

TG composition. TG species were fractionated by reversed-phase high-performance liquid chromatography (HPLC) on two columns of Lichrospher 100 RP 18 250 × 4 mm (Merck, Darmstadt, Germany) mounted in series, with a gradient of chloroform in acetonitrile (30:70 to 50:50 in 70 min). TG were quantified using an evaporative light-scattering detector Sedex 55 (SEDERE, Alfortville, France). Results were calculated from peak surface (S in $\mu V \cdot s$) using Equation 1 to take into account the nonlinearity of detector response:

$$S = 4300 \cdot M^{1.604} \quad [1]$$

where M is the mass of product in μg.

Fatty acid composition. After transmethylation as described by Morrison and Smith (27), fatty acids were analyzed by gas chromatography on a capillary column (J&W Scientic Inc., Folsom, CA; Type DB 225, 30 m × 0.32 mm) with a temperature gradient from 50 to 220°C. Results were expressed in percentage of peak surface.

Free fatty acids, monoacylglycerols, and diacylglycerols quantification. These components were analyzed as trimethylsilyl derivatives by gas chromatography on a capillary column (J&W Scientific; DB 5 HT, 15 m × 0.32 mm) with a temperature gradient from 100 to 350°C.

Phospholipids quantification. Phospholipids were quantified by colorimetric phosphorus determination in total lipid extract after acidic hydrolysis according to Bartlett (28). The coefficient used between phospholipids and phosphorus was 25.

Mixtures of CB and miglyol. Miglyol was added in increasing proportions to CB. All combinations of CB and miglyol, expressed in percentage (w/w), were thoroughly mixed in the liquid state at 70°C.

Thermal analysis. Thermal behaviors of CB, miglyol, and CB/miglyol mixtures were monitored by DSC using a DSC-7

PerkinElmer (St. Quentin en Yvelines, France). Samples were loaded in aluminum pans of 50 µL (pan, part #B014–3021 and cover, part #B014–3004) and hermetically sealed. An empty, hermetically sealed aluminum pan was used as reference. Calibration was made with lauric acid (m.p. 43.7°C, ΔH_m = 35.7 kJ/mol, purity >99.9%) so that temperature and enthalpies could be corrected, as previously described (29). Crystal memory was destroyed by maintaining the temperature of the samples at 60°C for 5 min. Crystallization behaviors were monitored with the temperature scanning program set from 60 to –50°C at 0.5°C/min for CB/miglyol mixtures and at 0.2, 0.5, 1, 2, 3 and 5°C/min for CB 75%/miglyol 25% mixture. Melting behaviors were monitored from –50 to 60°C at 2°C/min.

Structural analysis. Characterizations of CB, CB 75%/miglyol 25% mixture, and oil/water emulsions were conducted with an instrument allowing simultaneously time-resolved XRD with high-sensitivity DSC on the same apparatus from the same sample. XRD as a function of temperature (XRDT) was monitored with the high-energy synchrotron beam at LURE (Laboratoire pour l'Utilisation du Rayonnement Electromagnétique, Orsay, France) on two different benches. On a D22 bench, two linear detectors allowed XRD data collection at small and wide angles with sample-to-detector distances of 177.4 and 30 cm, respectively. On a D24 bench, a single detector, placed at 90 cm from the sample, allowed recording of XRD data at small angles. Both installations were equipped with a calorimeter that has been described elsewhere (30). All XRD patterns were recorded by transmission using thin glass capillaries (GLAS, Berlin, Germany) especially designed for XRD since they allow minimal attenuation of the beam and parasitic scattering (30). Samples were loaded by filling these glass capillaries with about 25 µL of melted fats or emulsion. X-ray patterns were taken every minute during about 59 s. Each frame represent an averaged XRD pattern recorded during 59-s temperature scan (step is 0.5°C on cooling). Channel to scattering vector **q** ($q = 4\pi$; $\sin(\theta)/\lambda = 2\pi/d$; q in Å^{-1}, θ in degrees is the angle of incidence of X-ray relative to the crystalline plane, λ is the X-ray wavelength, d in Å is the repeat distance between two reticular plans) calibration of the detectors was carried out at wide angles with the β form of high-purity tristearin, characterized by short-spacings of 4.59, 3.85, and 3.70 ± 0.01 Å (31), and at small angles with silver behenate characterized by a long-spacing of 58.380 ± 0.001 Å (32). XRD patterns were analyzed using PEAKFIT software (Jandel Scientific, Erkrath, Germany) to determine the position, the maximal intensity of the peaks, and the area under the peaks. X-ray peaks were fitted by a Gaussian-Lorentzian (sum) equation as described elsewhere (33).

Fractionation. The CB 75%/miglyol 25% mixture was heated at 70°C during 10 min in order to eliminate all the crystals and nuclei. The sample was cooled at 0.5°C/min. until 17°C. Then, centrifugation of the sample at 19°C ± 2°C during 1 min allowed the upper liquid phase to separate from the lower crystallized phase. The crystallized phase was washed with hexane in order to eliminate liquid TG between crystals. Hexane was evaporated under vacuum with nitrogen. The two fractions were analyzed by HPLC in order to determine their TG composition (see above).

Emulsion preparation. The aqueous phase consisted of distilled water, NaCl 80 mM, and 0.04 wt% sodium azide as a preservative. Protein solution was prepared by adding 4 wt% β-lactoglobulin powder (Laiterie Triballat, Noyal sur Vilaine, France) to the aqueous phase and then stirring overnight at room temperature to ensure complete dispersion of the protein. The pH of protein solution was adjusted to 6.7 with 1 M NaOH. CB 75%/miglyol 25 mixture was melted at 60°C during 30 min. Model fat and protein solution were mixed at 60°C to give 45% (vol/vol) oil in the final emulsion. Emulsion premix was prepared using the rotor stator system Polytron PT 3000 (Kinematica, Littau, Switzerland) equipped with a 12-mm head working at 20,000 rpm for 30 s. Homogenization of the coarse emulsion was then achieved at 10 bar with a high-pressure valve homogenizer (Stansted Fluid Power, Stansted, United Kingdom).

Droplet-size distribution. After homogenization, 1 mL of the emulsion was diluted into 9 mL of a sodium dodecyl sulfate solution (sodium dodecyl sulfate 1%, NaCl 80 mM, pH 6.7). This dilution ensures complete deflocculation of the oil droplets. The oil droplet-size distribution was measured by laser light-scattering using a Malvern Mastersizer (Malvern Instruments, Malvern, United Kingdom). The system was equipped with a lens of 45-mm focal length, and the manufacturer's presentation code 0505 was selected to take into account the refractive index of the oil. The mean droplet size ($d_{32} = \Sigma\, n_i d_i^3 / \Sigma\, n_i d_i^2$, where n_i is the number of droplets with diameter d_i) was d_{32} = 1.12 ± 0.03 µm.

RESULTS AND DISCUSSION

The objective of this work is to define a model fat allowing the study of crystallization in emulsion, by mixing of medium- and long-chain TG. The thermal and structural behaviors of CB and miglyol alone are studied first before that of their mixtures. The resulting best proportion mixture is then characterized and tested as an emulsion.

Characterization of CB and miglyol. (i) Composition. CB is mainly composed of TG (96.4%), but it also contains minor components as free fatty acids (1.8%), monoacylglycerols (0.2%), diacylglycerols (1.3%), phospholipids (0.1%), and sterols (0.2%). TG compositions of CB and miglyol are presented in Table 1. The TG composition found for CB, in which the monounsaturated species, mainly composed of POP (16.3%), POSt (34.8%) and StOSt (25.8%), represent a total of 79.0%, is in agreement with the literature. Miglyol is mainly composed of four TG with saturated medium chain-length acylglycerols with 8 and 10 carbon atoms (caprylic/capric acid TG) (about 1% of other fatty acids chains, caproic and lauric acids, were also found).

(ii) Thermal behavior. Crystallization and melting behaviors of both CB and miglyol were analyzed by recording DSC curves on cooling at 0.5°C/min, followed by a heating at 2°C/min (Fig. 1). This cooling rate was defined after a first study of the crystallization in emulsion (Lopez, C., G. Keller, A. Riaublanc, P. Lesieur, and M. Ollivon, unpublished results).

TABLE 1
Concentration of Triacylglycerols (TG) in Cocoa Butter (CB) and Miglyol (wt%)[a]

CB				Miglyol	
TG	%	TG	%	TG	%
OLO	0.5	StLSt	2.6	$C_yC_yC_y$	20.7
PLO	0.6	POSt	34.8	C_yC_yC	47.0
PLP	2.3	PPSt	1.4	C_yCC	28.4
OOO	0.7	StOSt	25.8	CCC	3.8
POO	2.5	PStSt	1.3		
PLSt	4.2	StOAr	2.0		
POP	16.3	StStSt	0.9		
StOO	3.4				
Saturated TG			3.6		99.9
Monounsaturated TG			79.0		—
Polyunsaturated TG			17.4		—
Total			100		99.9

[a]Abbreviations: Ar, arachidic acid (C20:0); L, linoleic acid (C18:2); O, oleic acid (C18:1); P, palmitic acid (C16:0); St: stearic acid (C18:0); C_y, caprylic acid (C8:0); C, capric acid (C10:0).

In this condition, crystallization of CB can be divided into three distinct exothermal events, with a total enthalpy ΔH_c = 94.2 J/g. The first exotherm spans from 23.3 (onset temperature) to 19.5°C. A second exothermal event, not distinctly separated, is recorded with an extrapolated onset temperature determined at 21.7°C. The major exothermal event recorded during cooling begins at 17.1 and finishes at 10.3°C (end temperature). DSC signal extends to about –5°C. On heating at 2°C/min, at least four endothermic events are recorded until final melting of all CB TG at 30.3°C (end temperature).

Crystallization of miglyol occurs in a single exotherm, with ΔH_c = 98.6 J/g, characterized by a temperature onset of –10.1 and an ending temperature of –19.2°C. The melting behavior of miglyol is more complex than crystallization since three distinct endothermal events are recorded until the final melting of TG at 2.25°C. DSC recordings demonstrate that CB and miglyol TG crystallize and melt in well-separated temperature domains. Thus, a very limited intersolubility in the solid state of both TG fat mixtures is expected.

(iii) Crystalline species formed by CB TG. Crystallization of CB was monitored at 0.5°C/min between 45 and –7°C by coupled XRDT and DSC experiments. XRDT patterns recorded at small and wide angles as a function of time during cooling are presented in Figure 2 as a three-dimensional view.

At small angles (Fig. 2), no diffraction lines are recorded for $T > 23$°C, meaning that all TG are in their liquid state. For $T \leq 23$°C, two diffraction lines are successively recorded at q = 0.129 Å^{-1} (48.6 Å) and q = 0.115 Å^{-1} (54.3 Å) with their superior orders of diffraction. At the end of the cooling, an increase of the X-ray signal near q = 0.14 Å^{-1} is also recorded.

XRDT patterns recorded at wide angles (Fig. 2, insert) show first a broad peak centered at q = 1.36 Å^{-1} (4.6 Å) corresponding to scattering signal of liquid TG (34). From about 22°C, a single peak of diffraction occurs and increases in intensity until the end of the experiments at –7°C. This peak,

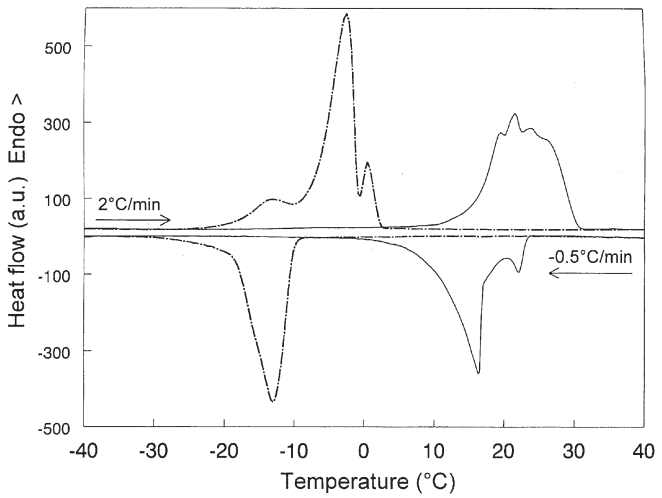

FIG. 1. Thermal behaviors of cocoa butter CB (—) and miglyol (— - —) conducted by differential scanning calorimetry (DSC) with a DSC-7 (PerkinElmer, St. Quentin en Yvelines, France). Crystallization curves were recorded at 0.5°C/min; following melting curves were recorded at 2°C/min.

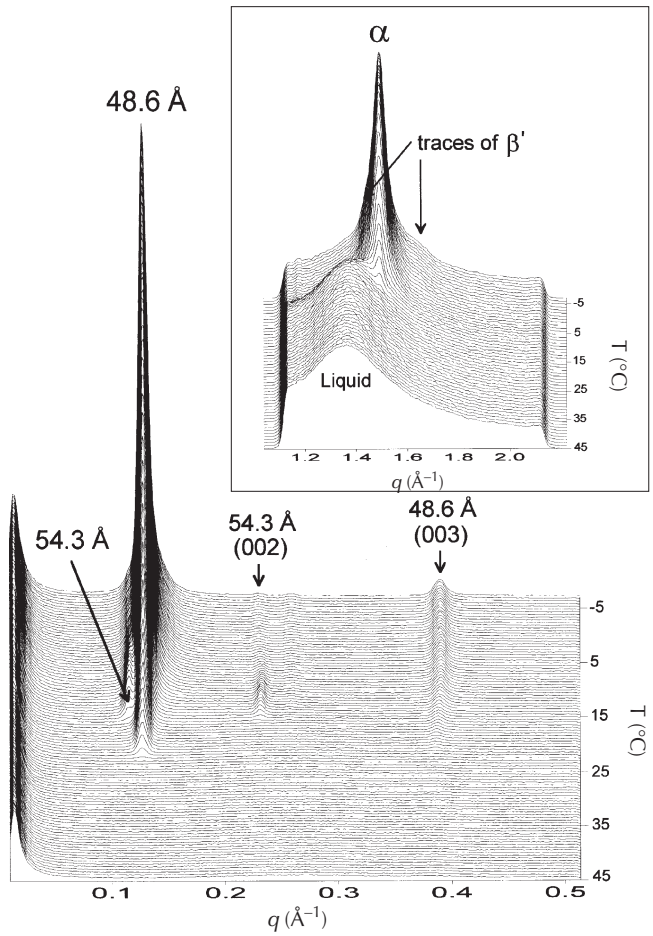

FIG. 2. Three-dimensional plots showing the evolution of the long- and short- (inset) spacings of CB as determined by small- and wide-angle X-ray diffraction (XRD), respectively, during cooling from 45 to –7°C at 0.5°C/min. The peaks characterizing the α and β′ packings are noted at wide angles (insert), while the long-spacings are labeled at small angles with their superior order of reflections (Miller index, *hkl*, with l = 2 or 3). See Figure 1 for abbreviation.

centered at q = 1.494 Å^{-1} (4.20 Å), is characteristic of a hexagonal packing of the acylglycerol chains, also called α form. X-ray bumps recorded at q = 1.46 Å^{-1} (4.30 Å) and 1.63 Å^{-1} (3.85 Å) likely correspond to small amounts of β′ form. At T ~ 18°C, the intensity of the maximum of the scattering peak suddenly decreases in intensity meaning that a liquid → solid TG transition occurs.

The evolution of maximal intensity of the main lines recorded at small and wide angles was analyzed using PEAKFIT (Table 2) and plotted as a function of temperature in order to delimit the domains of existence of the species. These data were compared to DSC crystallization curves recorded simultaneously (Fig. 3).

The increase in intensity of the major diffraction line recorded at small angles (Fig. 3A) can be divided into three temperature-delimited domains. For 23 ≥ T ≥ 19°C, the peak, the long-spacing of which is 49.2 Å, linearly increases in intensity (r^2 = 0.997; slope = –4.28%/°C) and stabilizes (see below). In the 18.5 ≥ T > 10°C domain, the intensity of the line increases linearly but with a steeper slope (r^2 = 0.998; slope = –7.93%/°C). Furthermore, the mean long-spacing of the variety in this domain decreases to 48.6 Å. Finally, for 9.5 ≥ T > –7°C, the line slowly increases in intensity and stabilizes. The main increase in intensity of the diffraction line corresponds to the progressive crystallization of CB TG (mainly monounsaturated TG) in a double-chain length organization (2L).

The evolution in intensity of the second crystalline variety formed by CB TG on cooling can also be divided into three domains (Fig. 3A). From its occurrence at 16 to 13.5°C, the diffraction line recorded at 54.3 Å rapidly and linearly increases in intensity (r^2 = 0.997; slope = –29.7%/°C), meaning that TG likely crystallize in a liquid crystalline organization (LC) (24). No other TG arrangement was found to explain the occurrence of this spacing, which is too short for a 3L and too long for a 2L packing since even the extended α conformation of tristearin is only 50.7 Å. Then, the intensity of this line linearly decreases (r^2 = 0.995; slope = 25%/°C) in the 13 > T > 11°C domain and continues to slightly decrease until the end of the experiment. The sums of peak areas of first orders allowed us to estimate the amount of this variety to be about 7% at T ~ 15°C. In the 13 > T > –7°C domain, the decrease in intensity of the 54.3 Å (LC) line and the simultaneous increase of the 48.6 Å (2L) line indicate that the LC variety progressively transforms to the benefit of the 2L variety. This behavior is attributed to a LC → 2L phase transition.

The evolution as a function of temperature of maximal intensity of the single line (4.20 Å) recorded at wide angles and attributed to the formation of a hexagonal chain packing is shown in Figure 3B. The occurrence of this first lateral organization of acylglycerol chains at about 22°C is correlated with the formation of the 2L variety recorded at small angles. The intensity of this line increases until about 13°C; then it stabilizes. Van Malssen *et al.* (23) showed that cooling of CB at 0.5°C/min results in α-crystallization only. The real-time X-ray powder diffractometer that they used, measuring d-spacings from 3.0 to 6.1 Å, allowed them to identify characteristic short-spacings but likely prevented them from obtaining information on the longitudinal organization of the TG molecules.

A crystallization curve recorded by DSC simultaneously with XRDT experiments on the same sample of CB is presented in Figure 3C. This DSC curve is similar to the one recorded with a DSC-7 (PerkinElmer) (Fig. 1). The analysis of XRDT data allows us to correlate thermal events to structural changes. The first exothermal event corresponds to crystallization of the first lamellar variety formed by TG in CB, corresponding to an α 2L organization with a thickness of 49.2 Å. Davis and Dimick (35) identified the lipid composition of high-melting seed crystals that promote the crystallization of CB. Seed crystals formed under static conditions contain high concentration of minor components such as phospholipids (6.6%), glycolipids (11.1%) and saturated TG, PPSt, PStSt and StStSt (82.4%). Then the first peak recorded by DSC on cooling is attributed to crystallization of highly

TABLE 2
Structural Parameters Obtained by X-ray Diffraction at Characteristic Temperatures for CB and CB 75%/Miglyol 25% Mixture on Cooling at 0.5°C/min[a]

CB					CB 75%/miglyol 25%				
T (°C)	LS (Å)	Type	SS (Å)	Type	T (°C)	LS (Å)	Type	SS (Å)	Type
23	49.2	2L	—	—	20.1	49.7 (s)	2L	4.18	α
22	49.2	2L	4.20	α	17	49.4 (s)	2L	4.18	α
18.5	49	2L	4.20	α	12.7	49.3 (s)	2L	4.20	α
16	48.7	2L	4.20	α		44.5	2L	3.87	β'_2
	54.3 (w)	LC				34.5	2L	4.27	
13.5	48.6	2L	4.20	α				4.15	β'_1
	54.3 (w)	LC						4.33	
10	48.6	2L	4.20	α	–8	49.3 (w)	2L	3.83	β'_2
	54.1 (w)	LC				44.5	2L	4.26	
–7	48.6	2L	4.20	α		34.5	2L	4.14	β'_1
	54.1 (w)	LC	3.84 (w)	β′				4.34	
			4.32 (w)						

[a]LS, long-spacings; SS, short-spacings; s, strong; w, weak, 2L, double-chain length; LC, liquid crystalline. For other abbreviation see Table 1.

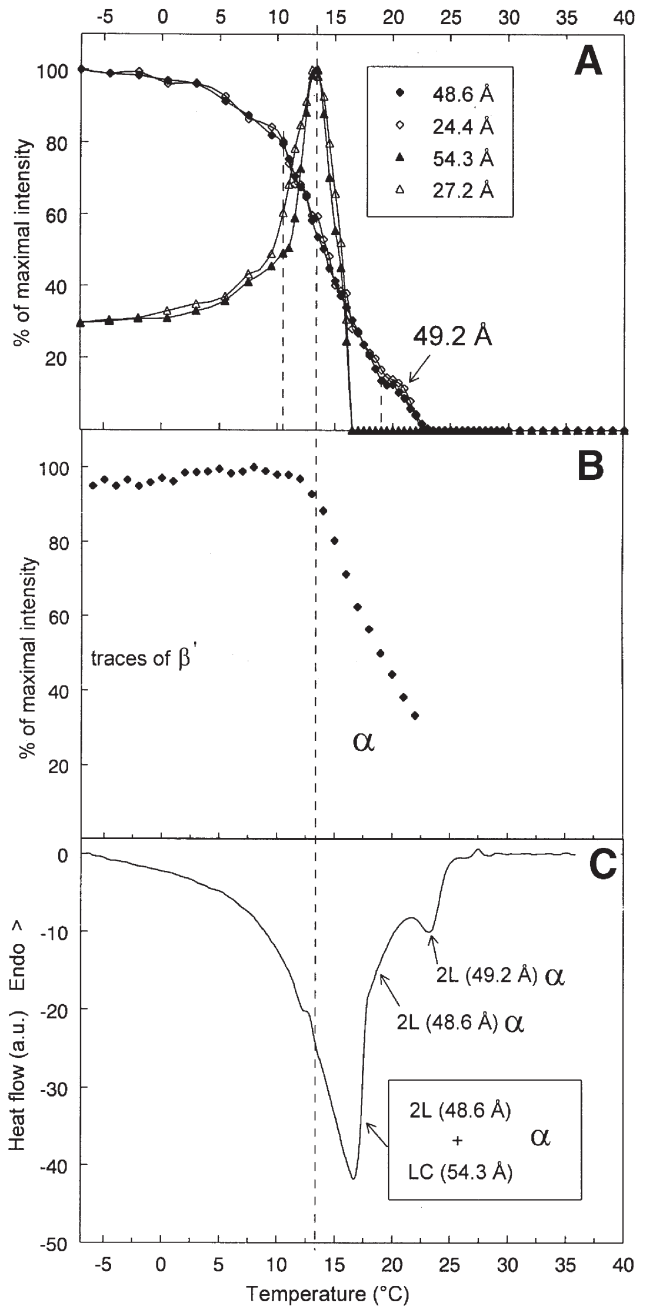

FIG. 3. Coupled X-ray diffraction as a function of temperature (XRDT) and DSC recordings. Evolution as a function of temperature of the maximal intensity of the main long- (A) and short- (B) spacings recorded in Figure 2, respectively, at small and wide angles during the cooling of CB at 0.5°C/min. Panel (C) represents the crystallization curve recorded simultaneously by DSC. See Figure 1 for other abbreviations.

saturated TG species (24). The second and major exothermal events are attributed to crystallization of monounsaturated TG in an α 2L (48.6 Å) form. Although the amount of 54.3 Å (LC) phase is much less important than that of the 48.6 Å one according to small-angle XRD (SAX), surprisingly the steep increase of the DSC exothermic peak starting at about 17.5°C coincides with the growth of the former. However, this steep increase cannot entirely be attributed to the simple 54.3 Å (LC) variety growth. Then the existence of a relationship between the occurrence of the LC and that of the 2L variety at 48.6 Å, for instance the former giving birth to the latter while transforming into, could not be ruled out. Coupling of small- and wide-angle XRDT and DSC experiments on the same sample allows us to relate structural and thermal behaviors, to follow phase transitions, and to provide in some cases the attribution of thermal events to the right TG species.

Mixtures of CB and miglyol. (i) Influence of CB/miglyol ratio on TG crystallization. Crystallization behaviors of different mixtures of CB and miglyol were monitored by DSC (DSC-7; PerkinElmer) on cooling at 0.5°C/min in order to study the influence of miglyol on CB TG crystallization (Fig. 4).

As a function of the increase in miglyol in the mixture, we noted (i) the temperature at which initial TG crystallization occurs decreases (Table 3), (ii) the enthalpy of the first exothermal event corresponding to crystallization of CB trisaturated TG decreases, (iii) the increase of both the crystallization temperature and enthalpy of the exotherm recorded at $T < -10$°C and corresponding to crystallization of miglyol TG, and (iv) the enthalpies of crystallization (ΔH_c) measured in the $25 > T > -10$°C domain as a function of CB amount in the different mixtures are larger than theoretical enthalpies calculated (Fig. 4, inset). Reciprocally, crystallization enthalpy of miglyol TG observed at $T < -10$°C is less than the theoretical enthalpies directly calculated from the melting enthalpy of each fat (Fig. 4, inset). DSC results show that miglyol TG contribute to the crystallization enthalpy of CB. It seems evident that miglyol modifies the crystallization behavior of CB TG and that the two fats do not crystallize separately, but rather at least partially co-crystallize. As

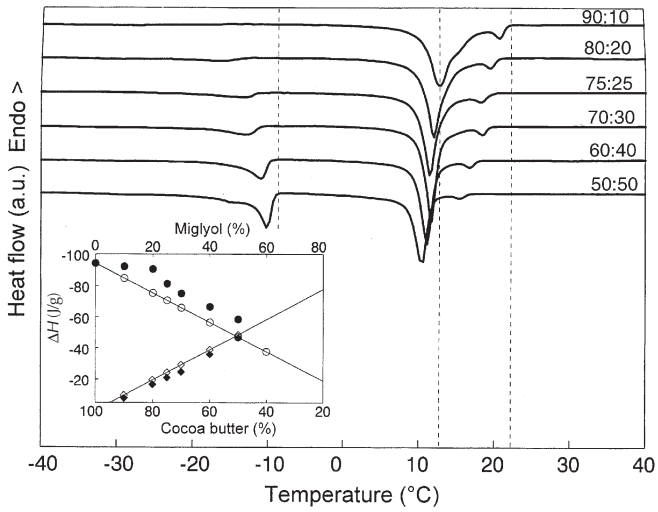

FIG. 4. Crystallization recordings of CB samples containing increasing amounts of miglyol recorded by DSC at 0.5°C/min. The proportions expressed as the ratio of CB/miglyol are indicated in the figure. Inset: evolution of the enthalpy of crystallization (ΔH, expressed in J/g) for $25 > T > -10$°C as a function of CB in the mixture (bottom x-scale) (○) theoretical ΔH, (●) measured ΔH; and for $T < -10$°C as a function of miglyol in the mixture (top x-scale) (◇) theoretical ΔH, (◆) measured ΔH. Theoretical ΔH were calculated in considering independent crystallizations of CB and miglyol, then linearly proportional to the crystallization enthalpies of pure compounds. See Figures 1 and 3 for other abbreviations.

TABLE 3
Evolution of Initial Crystallization Temperature (T_{onset}) as a Function of CB/Miglyol Mixtures During Cooling at 0.5°C/min[a]

CB/miglyol	T_{onset}
CB	23.3
90:10	21.8
80:20	20.7
75:25	19.7
70:30	19.4
60:40	17.9
50:50	16.7
Miglyol	–10.1

[a]For abbreviation see Table 1.

the miglyol TG crystallization started at about –8°C for the CB 50%/miglyol 50% mixtures, we decided to choose the CB 75%/miglyol 25% mixture as the model fat in order to avoid both miglyol and water crystallization at the lower limit of our emulsion studies, about –10°C.

(ii) Influence of DSC scanning rate. The crystallization behavior of the CB 75%/miglyol 25% mixture was studied as a function of cooling rate (R_c) (Fig. 5). For $1 \geq R_c \geq 0.2$°C/min, it was observed (i) that the same three exothermic events are recorded for $T > 0$°C (see above) and (ii) that a decrease of the initial crystallization temperature occurred as the cooling rate increased. For $R_c > 1$°C/min, the number of thermal events overlapping each other increases because of the complex polymorphism of this TG mixture. Furthermore, the narrowest crystallization range is obtained at 0.2°C/min; for higher cooling rates, the complexity of the curves increases with the crystallization range. The crystals obtained at different cooling rates may differ in polymorph forms or in chemical composition or both. DSC results show that the thermal behavior of this model fat is greatly dependent of the cooling rate used to characterize the sample.

In order to (i) separate the different solid phases formed during cooling, (ii) allow a full characterization by XRD, and (iii) have a good signal/noise ratio to study dispersed fat crystallization, we decided to conduct experiments on the model fat at 0.5°C/min cooling rate. In this condition, the fat system is extremely sensitive to nucleation and transition phenomena thanks to monotropic polymorphism of CB. Such sensitivity has already been used to study chocolate tempering, e.g., after chocolate tempering, less than 1% crystals of form V suffice to orient CB crystallization (36).

Structural and thermal behavior of the model fat: CB 75%/miglyol 25% mixture. (i) Crystallization behavior. Crystallization behavior of CB 75%/miglyol 25% mixture was studied on cooling between 50 and –10°C at 0.5°C/min by coupled XRDT and DSC experiments. The final temperature was chosen to allow a comparison with crystallization behavior of the model fat dispersed in emulsion (see below).

XRD patterns recorded simultaneously at small and wide angles as a function of time during cooling are presented in Figure 6.

On the three-dimensional view recorded at small angles (Fig. 6), three domains can be delimited in temperature. For $35 \geq T \geq 20$°C, all TG of the mixture are in the liquid state. In the $20 > T > 13$°C domain, a single diffraction line occurs and increases in intensity as a function of the decrease in temperature. For $T \leq 13$°C, two diffraction peaks are recorded with a simultaneous increase of the X-ray scattering at small angles ($0.02 < q < 0.13$ Å^{-1}).

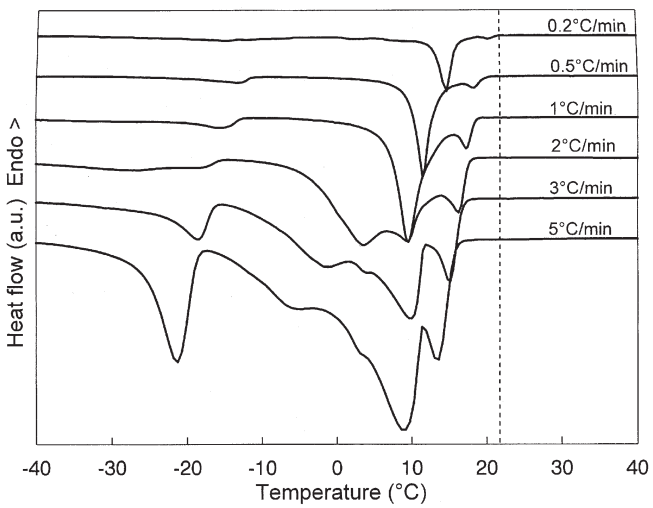

FIG. 5. Crystallization curves of the CB 75%/miglyol 25% mixture recorded by DSC at various cooling rates, as indicated in the figure. See Figures 1 and 3 for abbreviations.

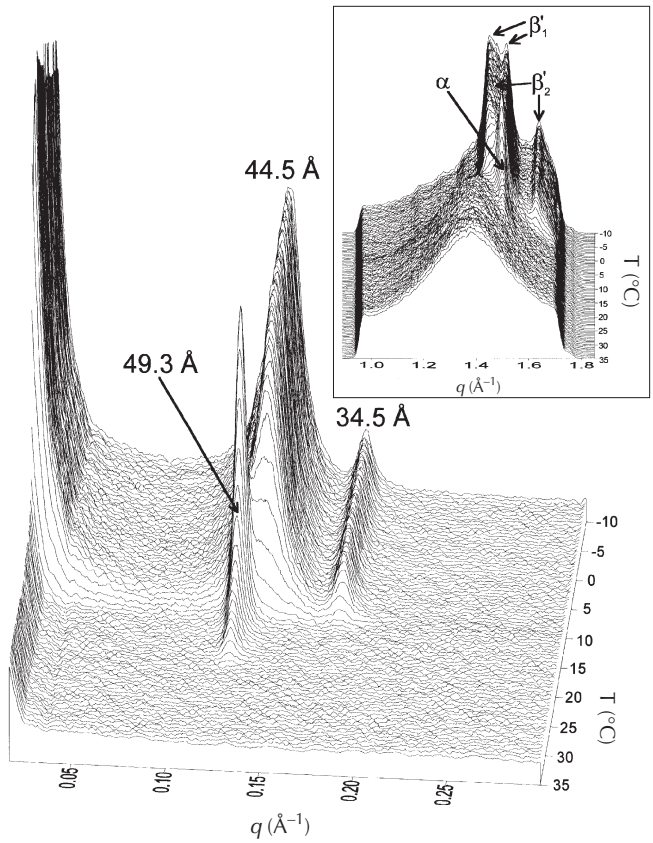

FIG. 6. Three-dimensional plots showing the evolution of the long- and short- (inset) spacings of the CB 75%/miglyol 25% mixture as determined by small- and wide-angle XRD, respectively, during cooling at 0.5°C/min. See Figures 1 and 3 for abbreviations.

On the wide-angle XRDT patterns recorded simultaneously with SAXD (Fig. 6, insert), a broad peak centered at q = 1.38 Å^{-1} (4.55 Å) corresponding to the organization of TG in their liquid state (likely LC) is first recorded (34). The progressive vanishing of this peak during cooling to the benefit of diffraction lines attributed to crystalline species confirms its identification. From about 20°C, a single line characteristic of a hexagonal packing (α) first develops, then lines corresponding to orthorhombic packing (β′) are recorded.

Each XRD pattern recorded at small and wide angles during cooling of the model fat at 0.5°C/min was analyzed using PEAKFIT in order to determine the position and the maximal intensity of each peak (Table 2, Fig. 7). The intensities of the diffraction lines determined as a function of temperature are normalized to their maximum to allow a comparison of the lines during cooling. Figures 8A and 8B show the evolutions plotted on the same graph of the maximal intensity of peaks corresponding, respectively, to long- and short-spacings. Such plots allow us to delimit the domains of existence of the crystalline species and to identify the phase transitions (37,38). Structural analysis obtained from XRDT data is correlated with thermal analysis recorded simultaneously by DSC (Fig. 8C).

On cooling at 0.5°C/min, a lamellar organization of TG with a long-spacing of 49.7 Å first occurs from about 20°C. The evolution in intensity of this line can be divided in three temperature-delimited domains. For 20 ≥ T ≥ 18°C, its increase in intensity is attributed to the formation of a double-chain length organization (2L). In this temperature range, the PEAKFIT analysis has shown that the long-spacing decreases from 49.67 to 49.44 ± 0.1 Å. The diffraction peak recorded simultaneously at wide angles at q = 1.5 Å^{-1} (4.19 Å) superimposed on the liquid-scattering signal corresponds to a hexagonal packing of the acylglycerol chains (α form). The parallel evolution of both sets of small- and wide-angle lines allows us to characterize a 2L (49.7 Å) α variety and to relate the formation of this crystalline organization to the first exothermal event recorded simultaneously by DSC (Fig. 8C). A complementary experiment consisted in separating the TG crystallizing in this first exotherm, in the 20–17°C range, by centrifugation (see Materials and Methods section). HPLC analysis allowed us to determine that the lipidic fraction that first crystallizes during cooling at 0.5°C/min of the CB 75%/miglyol 25% mixture is enriched in trisaturated TG ([PStSt] × 2.5) and ([StStSt] × 3.2) as observed in cacao butter (24, 35,39).

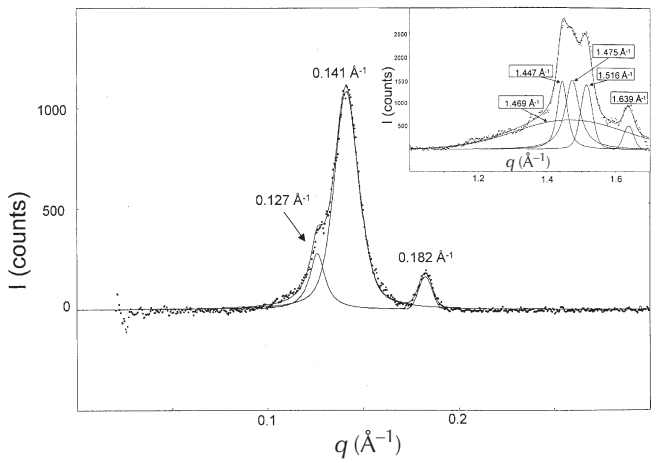

FIG. 7. PEAKFIT analysis of the XRD patterns recorded at both small and wide (inset) angles at –7°C (last pattern of Fig. 6). (●) are experimental values, (lines) are peak individual fits and their sum (global fit). Numbers on the figure correspond to the scattering vector q (Å^{-1}) measured at the top of each fitted peak. See Figures 1 and 3 for abbreviations.

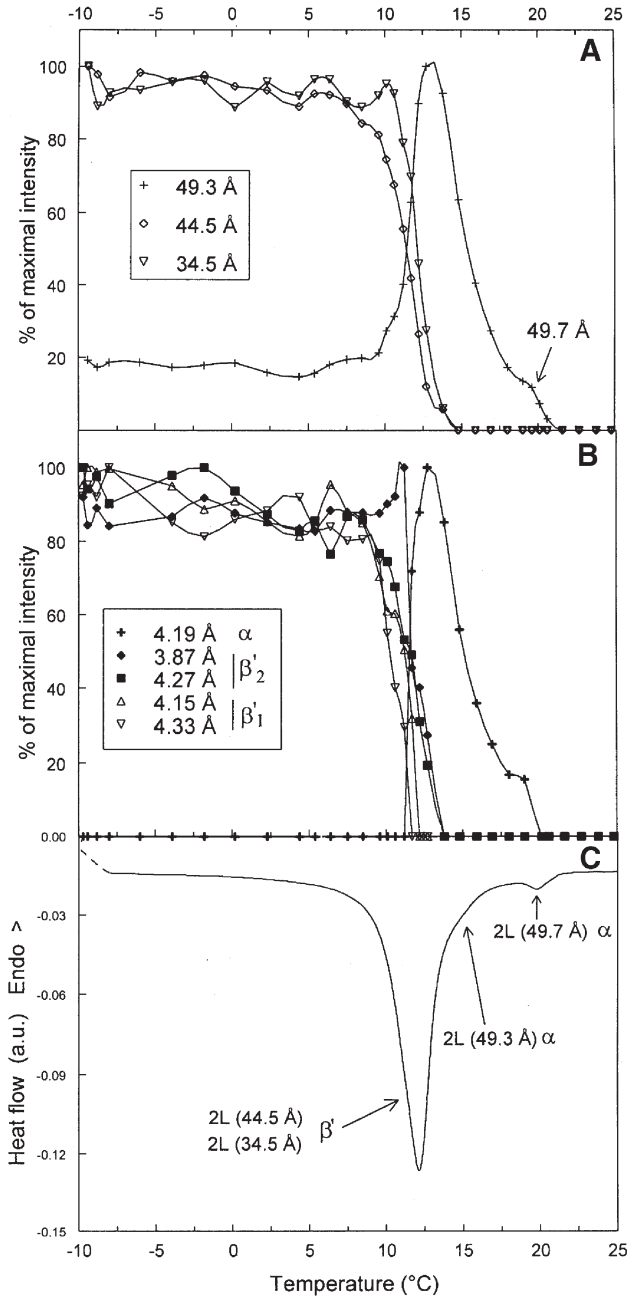

FIG. 8. Coupled XRDT and DSC recordings. Evolution as a function of temperature of the maximal intensity of the main long- (A) and short- (B) spacings recorded in Figure 6, respectively, at small and wide angles during the cooling of the CB 75%/miglyol 25% mixture at 0.5°C/min. Panel (C) represents the crystallization curve recorded simultaneously by DSC. See Figures 1 and 3 for abbreviations.

In the $17 \geq T \geq 12.7$°C domain, XRD data (Fig. 8A,B) clearly show the formation of the 2L (49.3 Å) α species, correlated with an exothermal event identified by DSC (Fig. 8C). The inflection point observed on both figures between about 18 and 17°C can be related to the growth of the new species.

For $12.2 \geq T \geq -10$°C, SAXD patterns show the complex X-ray signature of a lamellar organization characterized by two peaks corresponding to long-spacings of 44.5 and 34.5 Å and an increase of the scattered intensity at very small angles. The concomitant development of both 44.5 and 34.5 Å lines supports the hypothesis of a co-crystallization of two structures. This X-ray signature is correlated with the formation at wide angles of lines at 3.87 and 4.27 Å which correspond to an orthorhombic packing of TG attributed to a β'_2 form and lines at 4.15 and 4.33 Å corresponding to a β'_1 form. Figures 8A and 8B show that both long-spacing lines at 44.5 and 34.5 Å and the series of short-spacings develop simultaneously and display parallel evolutions. We deduced from the comparison of CB and CB 75%/miglyol 25% mixture crystallization behaviors (Figs. 2 and 6) that the presence of miglyol induces (i) an $\alpha \rightarrow \beta'$ transition, (ii) a 49.3 Å untilted $\rightarrow$ 44.5 Å tilted chain transition, both favored by the increase in liquid short-chain fatty acids in the mixture, and (iii) the formation of a "mixed structure" (see below) characterized by the line at 34.5 Å. The 44.5 and 49.3 Å lines can be related to β′ species corresponding to the forms IV and III of CB (22) (part of the line at 49.3 Å could be related to the presence of trisaturated TG in α form, as above). On the contrary, the line recorded at 34.5 Å was never observed for pure CB and was really puzzling. Indeed, such a period is not expected for CB, which is mainly composed of monounsaturated TG with 16–18 carbons per chain. Then, the line originates from either miglyol TG or a mixture of CB and miglyol TG. The period expected for miglyol crystallization in β′ form is about 25.3 Å [d (Å) = $2.32 \cdot n + 4.43$ Å, n being the mean carbon number per chain, here $n = 9$, (40)] (41). The 69 Å period (34.5 Å × 2) was ruled out. Then, we concluded that this line could not originate from a pure miglyol structure. Furthermore, such a structure is not expected at $T > 0$°C. Consequently, the line at 34.5 Å may only result from a CB–miglyol TG mixture as already suggested above from DSC experiments.

The average difference of chain length between miglyol and CB TG is about 8–9 carbons and largely exceeds the chain-miscibility limit in the solid state (41). Fatty acids of very different chain lengths likely segregate. The 34.5 Å chain length exactly corresponds to the sum of halves of 8–10 and 16–18 carbons per chain with about 24 and 44 Å chain lengths, respectively, measured for β′ packings (41). The thickness of the bilayer takes into account the void between glycerols. Then, all the data above suggest that a mixed packing that corresponds to a CB/miglyol 1:1 compound crystallizes in parallel with the form IV of the CB monounsaturated TG. Figure 9 shows such a possible structure in which both short- and long-chain fatty acids of TG segregate from fatty acid layer to fatty acid layer.

The rather intense scattering observed at low angles as well as the broadness of the main line might originate from (i) an imbrication of the two structures (phases) as found in alloys when both types of solid solutions near an eutectic composition crystallize almost simultaneously (co-crystallization) (42) and (ii) the small size of the crystals, or both. The fact that both phases crystallize simultaneously but melt at slightly different temperatures was interpreted as a mixture close to but not exactly at eutectic point. The relationship with the observation of a break point in the evolution of melting enthalpy vs. fat composition was not investigated (does this point correspond to a phase limit?). The whole CB–miglyol system needs further investigation for a complete understanding of the intermediate structures and thermal behaviors.

(ii) Melting behavior. The melting behavior of the CB 75%/miglyol 25% mixture crystallized at 0.5°C/min was followed on heating at 2°C/min using DSC/XRDT coupling (Fig. 10). The melting sequence as observed at both small (Fig. 10A) and wide (Fig. 10A, inset) angles was the following: First, the 49.3 Å variety melts at about 21°C, then, the 34.5 Å (2L β′) one at about 24°C before the major species at 44.5Å (2L β′) that vanishes around 30°C. A β phase, characterized by two long-spacings at 66 and 33 Å and a 4.6 Å line, forms around 20°C and melts at about 34°C. The fact the melting temperature of this β variety is almost unaffected compared with that observed for pure CB tends to support the nonmiscibility of both types of TG. The DSC curve recorded simultaneously (Fig. 10B) shows that the melting of the first three varieties cannot be distinguished one from the other while the β variety melting is clearly observed as a separate event.

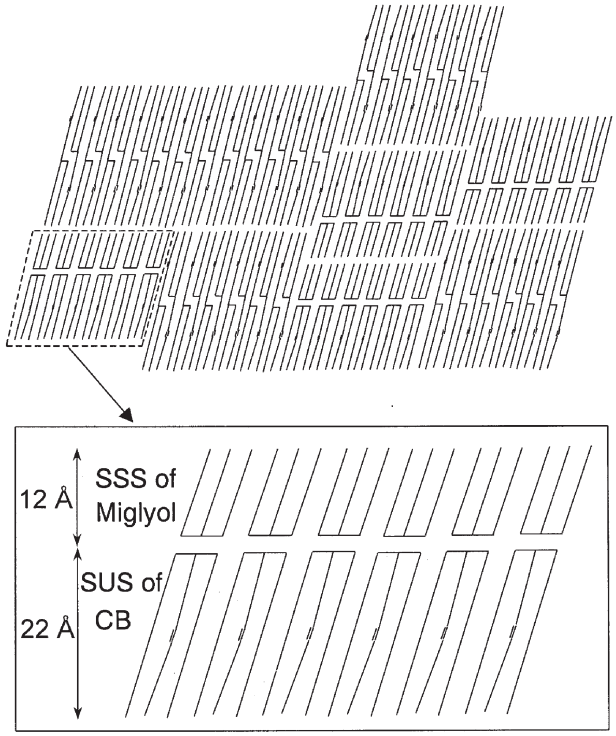

FIG. 9. Possible β′ packing model for trisaturated (SSS) miglyol and monounsaturated (SUS) CB mixed crystals corresponding to the 34.5 Å long-spacing measured by XRD (Fig. 6). See Figures 1 and 2 for other abbreviations.

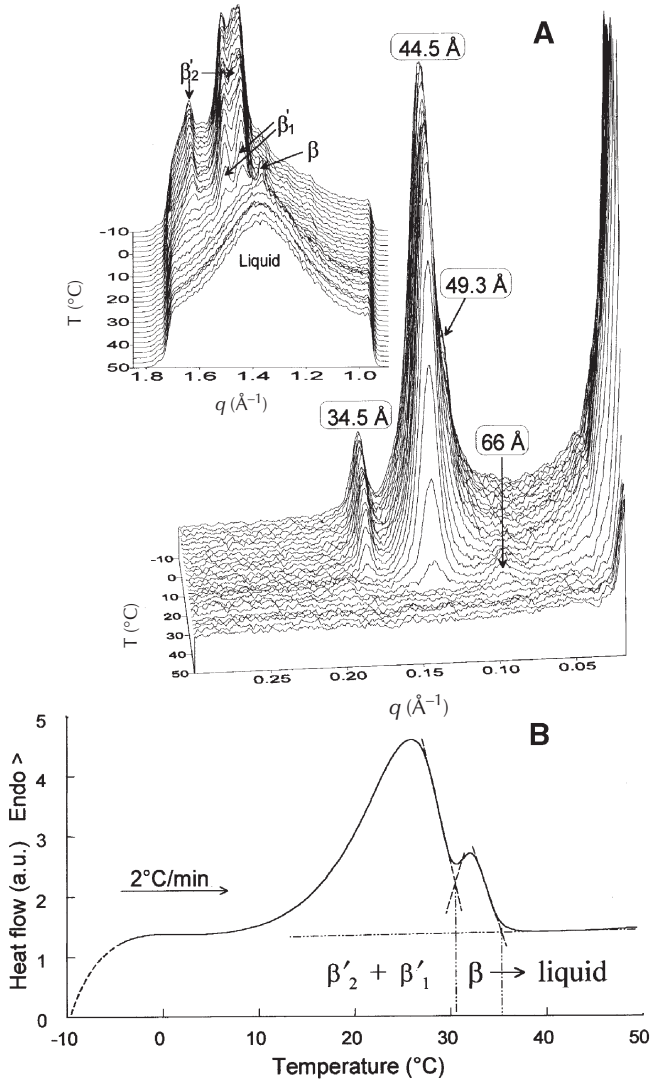

FIG. 10. Coupled XRDT and DSC recordings. (A) Three-dimensional plots recorded by XRD at small and wide (inset) angles during heating of the CB 75%/miglyol 25% mixture at 2°C/min (B) DSC melting curve recorded simultaneously. See Figures 1, 2, and 3 for abbreviations.

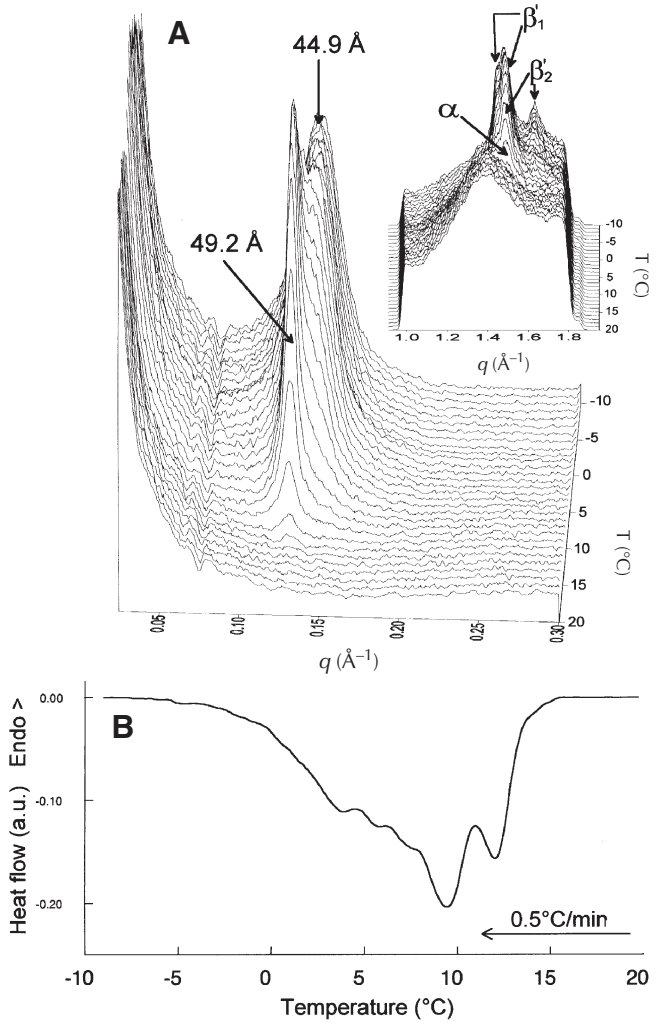

FIG. 11. Coupled XRDT and DSC recordings. (A) Three-dimensional plots of XRD patterns recorded at small and wide (inset) angles during cooling at 0.5°C/min of the model fat emulsion stabilized with β-lactoglobulin (the negative peak observed at about 0.07 $Å^{-1}$ is due to a detector defect). (B) DSC crystallization curve recorded simultaneously. See Figures 2 and 3 for abbreviations.

Crystallization of the model fat dispersed in emulsion. The model fat defined as the CB 75%/miglyol 25% mixture was dispersed in emulsion droplets (45% fat, vol/vol), with a mean diameter of 1.12 μm, stabilized by β-lactoglobulin. The low value of the average droplet diameter observed for a protein-stabilized emulsion is likely attributable to the presence of minor lipids originating from CB. Indeed, besides the fact that this model mixture offers the advantage to be easily obtained from commercial fats, the presence of small amounts of polar lipids in CB such as mono- and diacylglycerols and fatty acids might induce the formation of nucleation sites (14,43) which likely decrease the supercooling temperature range (44) as well as contribute to a mean droplet size reduction (45). However, the presence of such catalytic impurities in known amounts does not prevent the study of finely divided emulsions of various size in which large quantities of emulsifiers are added to stabilize (or destabilize) the emulsion (Lopez, C., G. Keller, A. Riaublanc, P. Lesieur, and M. Ollivon, unpublished data). In this respect, it is worth noting that emulsions made in the same conditions but from unblended CB were not stable below room temperature while those made from this model fat were stable for days or weeks.

The emulsion was characterized by coupled XRDT and DSC measurements during cooling at 0.5°C/min from 50 to –10°C. Crystallization behavior of TG dispersed in emulsion was not conducted below –10°C in order to avoid ice formation. The study of thermal and structural behavior of TG dispersed in emulsion is much more challenging than in bulk fat because of the presence of water that decreases the recorded signals by simple dilution effect. The three-dimensional plots of XRD patterns recorded simultaneously at small and wide angles are presented in Figure 11A. The occurrence of diffraction peaks corresponding to both the longitudinal stacking of TG (Fig. 11A) and lateral packing of acylglycerol

chains (Fig. 11A, inset) dispersed in droplets shows that XRDT experiments using synchrotron radiation allow us (i) to study TG crystallization within emulsion droplets, (ii) to identify crystalline species formed, and (iii) to follow their evolution as a function of temperature.

The DSC crystallization curve recorded simultaneously with XRDT measurements is shown in Figure 11B. Several overlapped exothermal events extend from the initial crystallization temperature of 13.6°C to about –7°C, where the DSC signal returns to the baseline. Compared to anhydrous fat, crystallization of the model fat dispersed in emulsion (i) starts with a more important supercooling $\Delta T = 19.7 - 13.6 = 6.1$°C, (ii) spans a larger temperature range, and (iii) exhibits a much more complex thermal behavior.

The thermal and structural behaviors of the model fat dispersed in emulsion have been analyzed, by coupled XRDT and DSC experiments, as a function of the type of protein used as an emulsifier, of the polar lipids associated with the proteins at interface and of the size of the emulsion droplets. It has been shown using this model fat that all these factors influence the crystallization behavior (Lopez, C., G. Keller, A. Riaublanc, P. Lesieur, and M. Ollivon, unpublished data).

ACKNOWLEDGMENTS

The authors thank ARILAIT Recherches, especially members of the steering committee, and ANRT (Association Nationale pour la Recherche Technique) for supporting this research. They also thank Christelle Leborgne (INRA-LEIMA) for analytical determinations.

REFERENCES

1. Jensen, R.G., and D.S. Newburg, Bovine Milk Lipids, in *Handbook of Milk Composition*, edited by R.G. Jensen, Academic Press, 1995, p. 542.
2. Swaisgood, H.E., Characteristics of Edible Fluids of Animal Origin: Milk, in *Food Chemistry*, edited by O.R. Fennema, Marcel Dekker, New York, 1985, pp. 791–828.
3. Tverdokhleb, G.V., and V.M. Vergelesov, Brief communication, in *XIX International Dairy Congress* 1^{E}, 1974, p. 211.
4. Timms, R.E., The Phase Behaviour and Polymorphism of Milk Fat, Milk Fat Fractions and Fully Hardened Milk Fat, *Aust. J. Dairy Technol. 35*:47–53 (1980).
5. Mulder, H., Melting and Solidification of Milk Fat, *Neth. Milk Dairy J. 71*:149–174 (1953).
6. de Man, J.M., Physical Properties of Milk Fat. II. Some Factors Influencing Crystallization, *J. Dairy Res. 28*:117–122 (1961).
7. de Man, J.M., Polymorphism in Milk Fat, *Dairy Sci. Abstr. 25*:219–221 (1963).
8. van Beresteyn, E.C.H., Polymorphism in Milk Fat in Relation to the Solid/Liquid Ratio, *Neth. Milk Dairy J. 26*:117–130 (1972).
9. Lavigne, F., Polymorphisme et transitions de phases des triglycérides. Applications aux propriétés thermiques et structurales de la matière grasse laitière anhydre et des ses fractions, Ph.D. Université Paris VII, Paris XI et E.N.S.I.A., 1995.
10. Marangoni, A.G., and R. Lencki, Ternary Phase Behavior of Milk Fat Fractions, *J. Agric Food Chem. 46*:3879–3884 (1998).
11. ten Grotenhuis, E., G.A. van Aken, K.F. van Malssen, and H. Schenk, Polymorphism of Milk Fat Studied by Differential Scanning Calorimetry and Real-Time X-Ray Powder Diffraction, *J. Am. Oil Chem. Soc. 76*:1031–1039 (1999).
12. Keenan, T.W., and D.P. Dylewski, Intracellular Origin of Milk Lipid Globules and the Nature and Structure of the Milk Lipid Globule Membrane, in *Advanced Dairy Chemistry Volume 2, Lipids*, 2nd edn., edited by P.F. Fox, Aspen Publishers, 1994, pp. 89–130.
13. Walstra, P., On the Crystallization Habit in Fat Globules, *Neth. Milk Dairy J. 21*:166–191 (1967).
14. Walstra, P., and E.C.H. van Beresteyn, Crystallization of Milk Fat in the Emulsified State, *Ibid. 29*:35–65 (1975).
15. Buchheim, W., and D. Precht, Electron Microscopic Study on the Crystallization Processes in Fat Globules During the Ripening of Cream, *Milchwissenschaft 34*:657–662 (1979).
16. Söderberg, I., L. Hernqvist, and W. Buchheim, Milk Fat Crystallization in Natural Milk Fat Globules, *Ibid. 44*:403–406 (1989).
17. Lopez, C., P. Lesieur, G. Keller, and M. Ollivon, Thermal and Structural Behavior of Milk Fat. 1. Unstable Species of Cream, *J. Colloid Interface Sci. 229*:62–71 (2000).
18. McClements, D.J., E. Dickinson, S.R. Dungan, J.E. Kinsella, J.G. Ma, and M.J.W. Povey, Effect of Emulsifier Type on the Crystallization Kinetics of Oil-in-Water Emulsions Containing a Mixture of Solid and Liquid Droplets, *Ibid. 160*:293–297 (1993).
19. Dickinson, E., F.-J. Kruizenga, M.J.W. Povey, and M. van der Molen, Crystallization in Oil-in-Water Emulsions Containing Liquid and Solid Droplets, *Colloids Surf. A 81*:273–279 (1993).
20. Özilgen, S., C. Simoneau, J.B. German, M.J. McCarthy, and D.S. Reid, Crystallization Kinetics of Emulsified Triglycerides, *J. Sci. Food Agric. 61*:101–108 (1993).
21. Pontillon, J., Sources et monographies des principauz corps gras, in *Manuel des corps gras*, edited by A. Karleskind and J.P. Wolff, Lavoisier, Paris, 1992, pp. 202–208.
22. Wille, R.L., and E.S. Lutton, Polymorphism of Cocoa Butter, *J. Am. Oil Chem. Soc. 43*:491–496 (1966).
23. Van Malssen, K., R. Peschar, and H. Schenk, Real-Time X-Ray Powder Diffraction Investigations on Cocoa Butter. I. Temperature-Dependent Crystallization Behavior, *Ibid. 73*:1209–1215 (1996).
24. Loisel, C., G. Keller, G. Lecq, C. Bourgaux, and M. Ollivon, Phase Transitions and Polymorphism of Cocoa Butter, *Ibid. 75*:425–439 (1998).
25. Sato, K., T. Arishima, Z.H. Wang, K. Ojima, N. Sagi, and H. Mori, Polymorphism of POP and SOS. I. Occurrence and Polymorphic Transformation, *Ibid. 66*:664–674 (1989).
26. Arishima, T., N. Sagi, H. Mori, and K. Sato, Polymorphism of POS. I. Occurrence and Polymorphic Transformation, *Ibid. 68*:710–715 (1991).
27. Morrison, W.R., and L.M. Smith, Preparation of Fatty Acids Methyl Esters and Dimethylacetals from Lipids with Boron Fluoride-Methanol, *J. Lipid Res. 5*:600–608 (1964).
28. Bartlett, G.R., Phosphorus Assay in Column Chromatography, *J. Biol. Chem. 234*:466–468 (1959).
29. Grabielle-Madelmont, C., and R. Perron, Calorimetric Studies on Phospholipid–Water Systems. I. DL-Dipalmitoylphosphatidylcholine (DPPC)-Water System, *J. Colloid Interface Sci. 95*:471–482 (1983).
30. Keller, G., F. Lavigne, L. Forte, K. Andrieux, M. Dahim, C. Loisel, M. Ollivon, C. Bourgaux, and P. Lesieur, DSC and X-ray Diffraction Coupling. Specifications and Applications, *J. Thermal Analysis 51*:783–791 (1998).
31. Ollivon, M., Triglycérides, in *Manuel des Corps Gras*, edited by A. Karleskind and J.P. Wolff, Lavoisier, Paris, 1992, p. 469.
32. Blanton, T.N., C.L. Barnes, and M. Lelental, Preparation of Silver Behenate Coatings to Provide Low- to Mid-Angle Diffraction Calibration, *J. Appl. Cryst. 33*:172–173 (2000).
33. Lopez, C., P. Lesieur, C. Bourgaux, G. Keller, and M. Ollivon, Thermal and Structural Behavior of Milk Fat. 2. Crystalline Forms Obtained by Slow Cooling of Cream, *J. Colloid Interface Sci. 240*:150–161 (2001).

34. Larsson, K., Molecular Arrangement in Glycerides, *Fette Seifen Anstrichm. 74*:136–142 (1972).
35. Davis, T.R., and P.S. Dimick, Lipid Composition of High-Melting Seed Crystals Formed During Cocoa Butter Solidification, *J. Am. Oil Chem. Soc. 66*:1494–1498 (1989).
36. Adenier, H., H. Chaveron, and M. Ollivon, Contrôle du tempérage du chocolat par analyse thermique différentielle simplifiée, *Sci. Aliments. 4*:213–231 (1984).
37. Kellens, M., W. Meeussen, C. Riekel, and H. Reynaers, Time-Resolved X-ray Diffraction Studies of the Polymorphic Behaviour of Tripalmitin Using Synchrotron Radiation, *Chem. Phys. Lipids 52*:79–98 (1990).
38. Lavigne, F., C. Bourgaux, and M. Ollivon, Phase Transition of Saturated Triglycerides, *Suppl. J. Phys. I. 3*:137–140 (1993).
39. Loisel, C., Physicochimie du chocolat: Cristallisation du beurre de cacao et propriétés structurales, Ph.D., Université Paris VII, Paris XI et E.N.S.I.A., 1996.
40. Ollivon, M., Contribution à l'étude des triglycérides. Polymorphisme et transitions de phases, Ph.D., Université Paris VII, 1982.
41. Small, D.M., *Handbook of Lipid Research. The Physical Chemistry of Lipids. From Alkanes to Phospholipids*, Plenum Press, New York, 1986.
42. Prince, A., Binary Phase Diagrams. Three-Phase Equilibrium Involving Limited Solubility of the Components in the Solid State but Complete Solubility in the Liquid State, in *Alloy Phase Equilibria,* Elsevier, Amsterdam, 1966, pp. 68–69.
43. Skoda, W., and van den Tempel, M., Crystallization of Emulsified Triglycerides, *J. Colloid Sci. 18*:568 (1963).
44. Phipps, L.W., Heterogeneous and Homogeneous Nucleation in Supercooled Triglycerides and *n*-Paraffins, *Trans. Faraday Soc. 60*:1873–1883 (1964).
45. Dickinson, E., Protein-Stabilized Emulsions, *J. Food Eng. 22*:59–74 (1994).

[Received March 19, 2001; accepted August 24, 2001]